Palaeogeography, Palaeoclimatology, Palaeoecology 528 (2019) 50–59

Contents lists available at ScienceDirect

Palaeogeography, Palaeoclimatology, Palaeoecology

journal homepage: www.elsevier.com/locate/palaeo

Anthropogenic ocean warming and acidification recorded by Sr/Ca, Li/Mg, δ^{11}B and B/Ca in *Porites* coral from the Kimberley region of northwestern Australia

Xuefei Chen[a,b,*], Juan Pablo D'Olivo[b,c], Gangjian Wei[a], Malcolm McCulloch[b,c]

[a] State Key Laboratory of Isotope Geochemistry, Guangzhou Institute of Geochemistry, Chinese Academy of Sciences, Guangzhou 510640, China
[b] Oceans Graduate School and Oceans Institute, The University of Western Australia, Crawley 6009, Australia
[c] ARC Centre of Excellence for Coral Reef Studies, The University of Western Australia, Crawley 6009, Australia

ARTICLE INFO

Keywords:
Coral calcification
Calcifying fluid
Carbonate chemistry
Boron isotopes

ABSTRACT

The impact of climate changes on corals living in naturally extreme environments is poorly understood but crucial to longer-term sustainability of coral reefs. Here we report century-long temperature (Sr/Ca and Li/Mg) and calcifying fluid (CF) carbonate chemistry (δ^{11}B and B/Ca) records for a long-lived (1919 to 2016) *Porites* coral from the high thermally variable Kimberley region of northwestern Australia. We investigate how increasing temperatures and ocean acidification are manifested in the carbonate chemistry of coral's CF and impacts of climate change on calcification. Using Sr/Ca and Li/Mg multiproxy we show that annual temperature in the nearshore Kimberley exhibited a gradual increase (0.009 ± 0.003 °C/yr) from the 1920s onward. However for the most recent years (2000–2015) more rapid summer warming (0.05 ± 0.01 °C/yr) are registered, indicative of intensified warming. Despite that, we find no significant trend for calcification rate of this coral over the past century, as well as 'normal' seasonal variability in coral's CF carbonate chemistry. Importantly, the coral's ability to concentrate inorganic carbon seems to be affected by recent warming, with reduced DIC_{cf} observed during 2008 to 2015, while the minimally-affected pH_{cf} acts to compensate the decreases of DIC_{cf} with the calcification rate showing only slight decrease. Additionally, we also find that ocean acidification has clearly led to the long-term reduction in the pH of the CF.

1. Introduction

Rising levels of CO_2 are driving both warming and acidification of the world's oceans (Rhein et al., 2013), posing significant and growing risks to the sustainability of coral reef ecosystems (Hughes et al., 2017). Thus, global warming acting together with severe and more frequent El Niño events (Cai et al., 2014) is now repeatedly subjecting coral reef ecosystems to thermally induced stress and resultant coral bleaching (Heron et al., 2016; Hughes et al., 2017; Spalding and Brown, 2015). However, it remains unclear whether corals living in naturally extreme thermal environments may potentially be better adapted to withstand the increasing effects of global warming, especially on decadal and longer timescales over which warming is occurring.

To evaluate longer-term responses of coral reefs to climate change is a challenging task due to the sparseness and shortness of instrumental records and observations of coral health. As calcification rate is the most perceptible expression of coral growth, it is commonly used to assess the major environmental controls and possible impacts of changing climatic conditions on coral performance (Cantin et al., 2010; Cooper et al., 2008, 2012; De'ath et al., 2009; D'Olivo et al., 2013; Lough and Barnes, 1992, 1997; Tanzil et al., 2013). It has been shown that over longer timescales the response of coral calcification to climate change can vary significantly among different environments. For instance, a long-term declining calcification is found in the inner Great Barrier Reef while outer-shelf reefs show a trend of increasing calcification (D'Olivo et al., 2013). Different calcification responses are also evident on a global scale. In the temperate Western Australia, as the sea surface temperature (SST) increases, the average coral calcification rate show a modest rise over the past century (Cooper et al., 2012). In contrast, coral calcification in the central Red Sea has reduced by 18% from 1998 to 2008 relative to the 1976–1997 mean, which is believed to be affected by the increased thermal stress (Cantin et al., 2010). Therefore, it seems that calcification rate alone may not be conclusive enough to reveal the whole picture of coral long-term responses to

* Corresponding author at: State Key Laboratory of Isotope Geochemistry, Guangzhou Institute of Geochemistry, Chinese Academy of Sciences, Guangzhou 510640, China.
E-mail address: chenxf@gig.ac.cn (X. Chen).

https://doi.org/10.1016/j.palaeo.2019.04.033
Received 28 February 2019; Received in revised form 30 April 2019; Accepted 30 April 2019
Available online 03 May 2019
0031-0182/

climate change. To better understand coral resilience in the changing world, more information remains to be extracted from corals. For example, the processes controlling the interaction between the changing marine environment and the biologically modulated controls on the composition of the coral extracellular calcifying fluid (CF) from which calcification occurs.

Skeletal geochemistry of scleractinian corals is sensitive to both external environment changes and the processes controlling internal biomineralization (Cohen and McConnaughey, 2003; Gagan et al., 2000; Gagnon et al., 2012; Trotter et al., 2011). Therefore, the geochemical information preserved within the skeleton of long-lived corals allows us to quantify coral responses to historic climate change. To assess the impacts of ocean warming on reef environment, coral Sr/Ca ratios serve as important tools to generate reliable temperature reconstruction where instrumental records are lacking (McCulloch et al., 1999; Smith et al., 1979). Additionally, the newly developed Li/Mg is another alternative SST proxy which is thought to be barely affected by Rayleigh fractionation as Mg^{2+} and Li^{+} have similar ionic sizes and partition coefficients ($K_D \ll 1$), and exhibits an approximately universal Li/Mg-T relationship regardless of species and environment (Fowell et al., 2016; Marchitto et al., 2018; Montagna et al., 2014). Furthermore, the combined $\delta^{11}B$ and B/Ca proxies offer a mechanistic approach to determine the carbonate chemistry of the coral CF, helping to unveil the key processes that control coral calcification (D'Olivo and McCulloch, 2017; McCulloch et al., 2017; Ross et al., 2018; Schoepf et al., 2017). Briefly, coral $\delta^{11}B$ proxy is thought to constrain the pH of the calcifying fluid (pH_{cf}) (Trotter et al., 2011; McCulloch et al., 2012a,b), while B/Ca ratios are an indicator for $[CO_3^{2-}]$ (Holcomb et al., 2016). With knowledge of these two parameters, the dissolved inorganic carbon (DIC) in the calcifying fluid (i.e. DIC_{cf}) can then be obtained (McCulloch et al., 2017). In tropical *Porites* spp. corals, $\delta^{11}B$ and B/Ca systematics indicate that corals can interactively up-regulate the DIC_{cf} and pH_{cf} in the CF in order to achieve higher aragonite saturation states, facilitating more rapid and stable rates of calcification (D'Olivo and McCulloch, 2017; McCulloch et al., 2017). This is achieved by doubling the DIC_{cf} compared to the seawater DIC (DIC_{sw}) and inversely varying levels pH_{cf} of from ~8.3 to ~8.5 that compared to seawater pH (pH_{sw}) of ~8.0 (McCulloch et al., 2017). Variations to these boron systematic records can therefore provide important mechanistic insights into coral responses to climate change.

In this study, we extracted both monthly- and annually-resolved geochemical records of Sr/Ca, Li/Mg, $\delta^{11}B$, and B/Ca from a long-lived (~100-year old) *Porites* coral living in the highly dynamic and thermally extreme nearshore Kimberley region of northwestern Australia. The main aim of this work is to investigate the effects of long-term high levels of thermal stress and the associated coral responses in terms of both calcification rate and its inorganic calcification mechanism. We provide new evidence of the ability of corals to up-regulate the carbonate chemistry at their site of calcification under mainly naturally occurring high-level conditions of thermal stress. By utilizing these coral-based geochemical proxies, we show that the impacts of climate change on highly fluctuating, naturally extreme temperature reef ecosystems can be evaluated, providing a better understanding of the resilience and responses of coral reefs in such environments.

2. Study area

The Kimberley region, located in the northernmost part of Western Australia (Fig. 1) , is a naturally extreme environment with abundant and highly diverse range of coral species as well as coral reef structures (Dandan et al., 2015; Richards et al., 2015; Rosser and Veron, 2011; Purcell, 2002; Schoepf et al., 2015). Corals from this region are regularly subject to high levels of thermal stress with mean monthly maximum sea surface temperature (SST) ranging from 31 °C (January to March) to 26 °C (July) (Dandan et al., 2015; Schoepf et al., 2015). Mean monthly SST > 30 °C can last for about 5 months (Dandan et al., 2015; Schoepf et al., 2015), regularly exceeding the typical coral growth optimum temperature for this environment (e.g., Schoepf et al., 2015). In addition, the highly dynamic tidal regimes of the Kimberley, which can exceed 12 m over a tidal cycle, can also lead to a large daily temperature variations of from ~30 °C to > 36 °C in summers, but with relatively small salinity changes (Dandan et al., 2015), with corals being frequently subjected to aerial exposure. Together these conditions have led to a highly variable thermal environment, for which corals have locally over time evolved adaptive mechanisms in order to sustain calcification and hence growth.

3. Materials and methods

3.1. Coral sampling

Coral core KIM16 was drilled in April 2016, from a living massive *Porites* spp. coral colony at a water depth of 2 m in low tide, on the subtidal zone of Shenton Bluff which is located on the lower reaches of King Sound (i.e., Cygnet Bay), Kimberley region of northwestern Australia (Fig. 1). The core was cut into slices (~7 mm thick) along the plane of the vertical growth axis, and X-rayed to reveal clear density and annual growth bandings that were used as a guide for sampling (Fig. S1). Before sampling, coral slabs were immersed in 6% reagent grade NaOCl for 24 h to remove organic material, followed with thoroughly rinse in an ultrasonic bath filled with deionized water, and then dried at 40 °C.

Both seasonal and annual samples were collected along the main growth axis using a computer controlled micromill. The top ~20 years (i.e. 1995–2015) of coral growth was milled at higher-resolution with samples being collected at continuous intervals of ~1.4 mm (i.e. ~8 subsamples per year). The sampling depth was set at a fixed value of ~0.8 mm to avoid lateral heterogeneity. The seasonally resolved geochemical data was then used to 'calibrate' the timing of the approximately annual (X-ray) density banding. Linear annual extension rates (1919 to 2015) were then measured across intervals of sub-parallel annual banding in the X-ray images and then used as a reference for the continuous sampling of annual increments down along the same milling path as seasonal subsamples.

3.2. Coral calcification rate

Coral calcification rate ($g\,cm^{-2}\,yr^{-1}$) was obtained by the product of the annual linear extension rate and the density. The linear extension rate was measured directly using the X-ray negative prints, and the skeletal density was measured along the maximum growth axis from X-ray prints with correction for intensity heterogeneity (Duprey et al., 2012).

3.3. Geochemical analyses

Elemental ratios (B/Ca, Sr/Ca, Li/Mg) were measured at approximately monthly (from 1995 to 2015) and annual (from 1919 to 2015) resolution. The geochemical measurements were undertaken at the University of Western Australia by Quadrupole Inductively Coupled Plasma Mass Spectrometer (Q-ICPMS, X-series II, Thermo Fisher Scientific) following the method described in Holcomb et al. (2015). About 10 mg of sample powder were dissolved in 0.51 M HNO_3, with sub-aliquots diluted in 2% HNO_3 to a final concentration of ~100 ppm Ca and 10 ppm Ca, respectively (the later spiked with Sc, Y and Pr used as an internal standard). All HNO_3 acid was prepared from sub-boiling distilled using a Davillex DST-1000. The ~100 ppm Ca solutions were prepared to measure ^{7}Li, ^{11}B, and ^{25}Mg while ~10 ppm Ca solutions for ^{25}Mg, ^{43}Ca, and ^{86}Sr. The remaining sample solution (400 µl) was then used for boron purification (described below). The coral standard JCp-1 (*Porites* spp.: Geological Survey of Japan) used as an internal standard for the measurements in our study yielded a mean Li/Mg value of

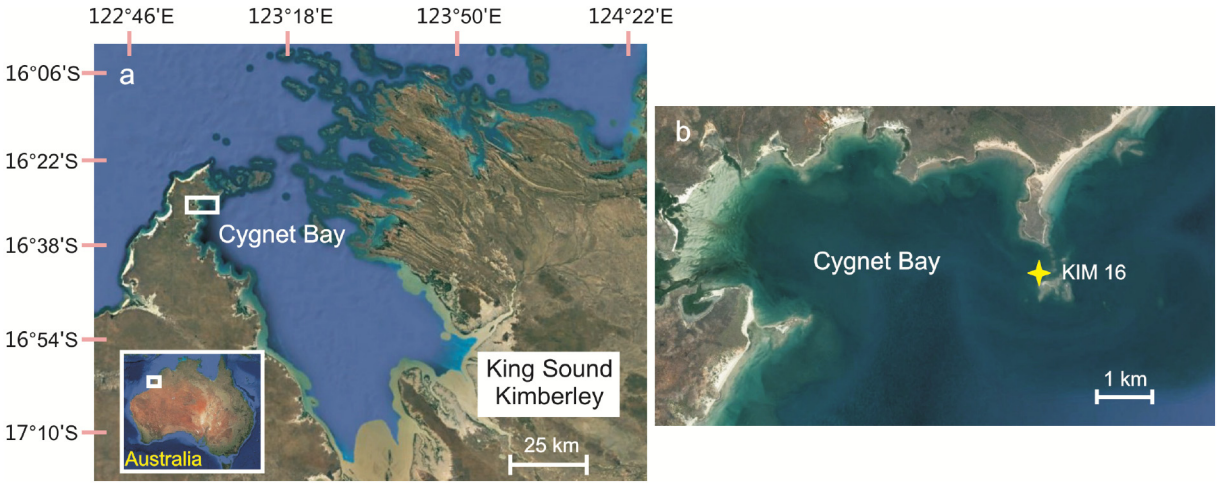

Fig. 1. (a) Location of the Cygnet Bay in King Sound, Kimberley region of northwestern Australia, (b) inset of the white box in (a). Yellow star indicates the sampling site. (For interpretation of the references to color in this figure legend, the reader is referred to the web version of this article.)

1.456 ± 0.027 (SD, $n = 15$) mmol/mol, Sr/Ca value of 8.848 ± 0.023 mmol/mol (SD, n = 15), and B/Ca value of 0.4565 ± 0.0238 (SD, n = 15) mmol/mol, which are all consistent with the values reported in Hathorne et al. (2013).

Boron isotopic composition was measured for the top 7-year seasonally resolved samples (2008 to 2015) and the annual samples representing the period from 1919 to 2015. The measurements were carried out using a Multicollector Inductively Coupled Plasma Mass Spectrometer (MC-ICPMS, NU Plasma II, Cameca instruments) at the University of Western Australia, following the methods described in McCulloch et al. (2014). A 400 µl aliquot from the dissolved sample was loaded onto the preconditioned cation and anion columns which contain 0.6 ml of AG50W-X8 resin and 1.0 ml of AG1-X8 resin, respectively, to remove both cation and anion matrix (e.g. Ca^{2+}, Sr^{2+}, and SO_4^{2-} ions) from the carbonate solution. The columns were then eluted with 4× 0.5 ml of 0.075 M HNO_3, yielding an ~200 ppb boron solution ready for $\delta^{11}B$ measurement using MC-ICPMS. Typical operating conditions and measurement strategies are summarized in McCulloch et al. (2014). Sample measurements were bracketed by ERM AE121 ($\delta^{11}B$ = 19.9 ± 0.6‰, BAM, Germany). Measurement of the coral standard JCp-1 that underwent the same chemically procedure as the coral samples yielded $\delta^{11}B$ values of 24.60 ± 0.12‰ (SD, $n = 10$), consistent with previously reported values within analytical errors (e.g. Foster et al., 2006; Gonfiantini et al., 2003; McCulloch et al., 2014; Wang et al., 2010).

3.4. Estimates for coral CF carbonate chemistry

The pH_{cf} is calculated from the coral skeletal boron isotopic compositions ($\delta^{11}B_{coral}$) according to the following equation (Zeebe and Wolf-Gladrow, 2001):

$$pH_{cf} = pK_B - \log\left[\frac{\delta^{11}B_{sw} - \delta^{11}B_{coral}}{\alpha_{B3-B4} \times \delta^{11}B_{coral} - \delta^{11}B_{sw} + 1000(\alpha_{B3-B4} - 1)}\right] \quad (1)$$

where $\delta^{11}B_{sw}$ is the B isotope composition of seawater ($\delta^{11}B_{sw}$ = 39.61‰, Foster et al., 2010) and the B isotope fractionation factor ($\alpha_{B3\text{-}B4}$) is 1.0272 estimated by Klochko et al. (2006). The B dissociation constant (pK_B) is well defined with a value of 8.597 at 25 °C and a salinity of 35 (Dickson, 1990a). The $[CO_3^{2-}]_{cf}$ is derived from B/Ca ratios according to the following relationship (Holcomb et al., 2016; McCulloch et al., 2017):

$$[CO_3^{2-}]_{cf} = K_D\,[B(OH)_4^-]_{cf}/[B/Ca]_{CaCO3} \quad (2)$$

where $[B(OH)_4^-]_{cf}$ is the concentration of borate in the CF estimated from the $\delta^{11}B_{coral}$, and K_D is the distribution coefficient for boron between aragonite and seawater. Details of boron geochemical proxies for carbonate chemistry are given in the electronic supplementary material.

Thus, with knowledge of pH_{cf} and $[CO_3^{2-}]_{cf}$, the complete carbonate system parameters, including $[DIC]_{cf}$, of the calcifying fluid can be determined. For our calculations we used carbonate species dissociation constants of Mehrbach et al. (1973) as re-fit by Dickson and Millero (1987), and the $KHSO_4$ from Dickson (1990b) and the aragonite solubility constants of Mucci and Morse (1983). Aragonite saturation state of the CF (Ω_{cf}) is calculated using $[CO_3^{2-}]_{cf}$ with the assumption that $[Ca^{2+}]_{cf}$ in *Porites* coral is about 8.3 mmol/kg (DeCarlo et al., 2017). Note that the newly developed coral Ω_{cf} Raman measurement indicates that $[Ca^{2+}]_{cf}$ also varies along with carbonate chemistry in CF, with values generally lower than seawater $[Ca^{2+}]_{sw}$ by ~11–25% for *Porites* corals (DeCarlo et al., 2017). Therefore, the calculated Ω_{cf} with fixed $[Ca^{2+}]_{cf}$ cannot fully resolve the variability of Ω_{cf}. Finally, the obtained Ω_{cf} and temperature were used to estimate the rates of theoretical calcification rate (G) according to the model of internal pH-regulation abiotic calcification (IpHRAC, McCulloch et al., 2012a,b) where the calcification rate is given by $G = k(\Omega_{cf} - 1)^n$ (Burton and Walter, 1987). The constants k and n are temperature dependent constant and order of the reaction, respectively.

4. Results and discussion

4.1. SST reconstruction

Although corals in the Kimberley are subject to highly variable and naturally extreme environmental conditions, the temperature-sensitive Sr/Ca and Li/Mg ratios do not appear to have been compromised by the highly dynamic hydrology and the intense thermal stress. Both elemental ratios exhibited strong seasonal cycles that closely followed the inter-annual variations in the temperature data obtained from the adjusted monthly Optimum Interpolation Sea Surface Temperature (OISST) records (see details in electronic supplementary material; Reynolds et al., 2007) (Fig. 2a&b). However, Li/Mg ratios exhibited noticeable offsets with the adjusted OISST for the 2014/15 section (the uppermost part of the core), which was largely induced by the greatly elevated Mg but little-affected Li contents (Fig. S3). The abrupt changes in coral skeletal Mg concentration may possibly relate to skeletal heterogeneity, diagenesis, heat stress, or contamination from organic materials (Clarke et al., 2017; Cuny-Guirriec et al., 2019; Lazareth et al., 2016; Meibom et al., 2008). In this case, since the anomalous increase in Mg abundance did not accompany with any changes in other

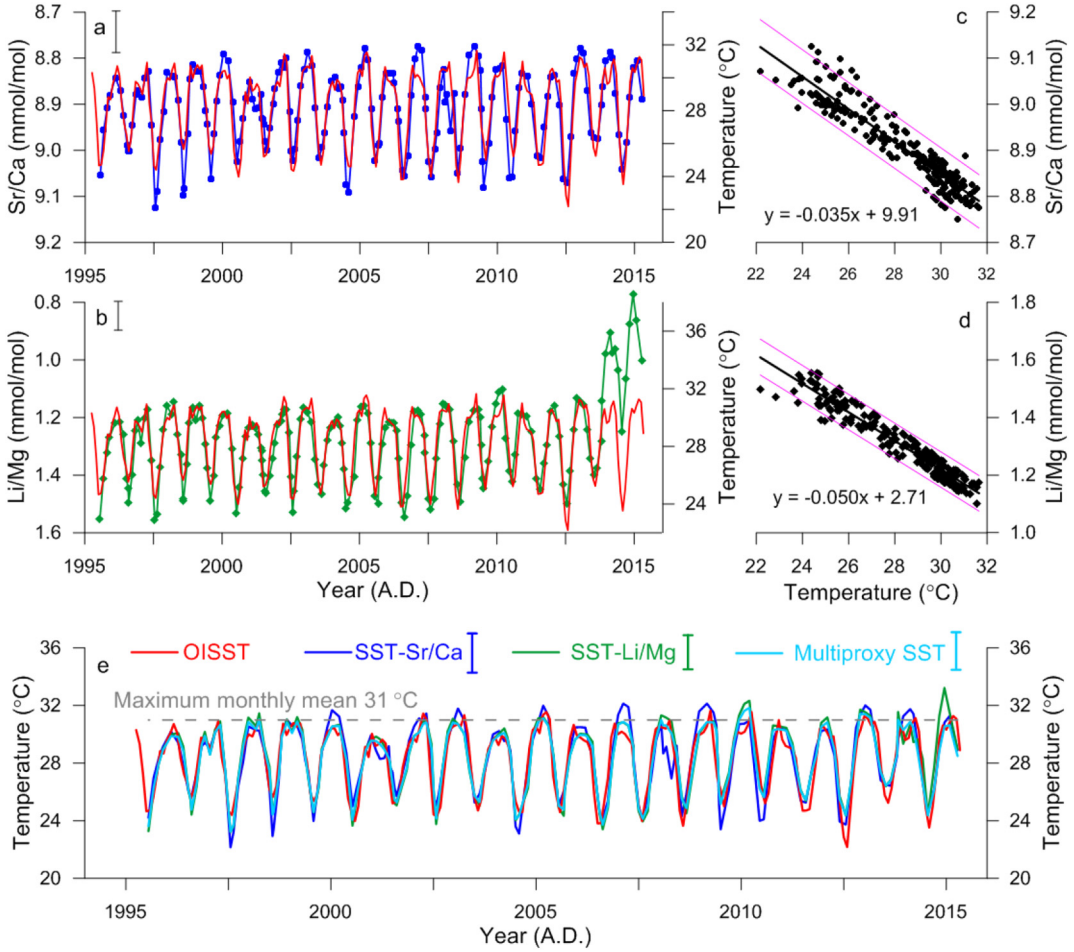

Fig. 2. Sr/Ca and Li/Mg ratios calibrations: a, Sr/Ca ratios (blue) vs. adjusted OISST (red); b, Li/Mg ratios (green) vs. adjusted OISST (red); c, liner regression analysis of Sr/Ca ratios and temperature ($r = -0.94$, $p(a) < 0.01$, $n = 238$) (1995 to 2015); d, linear regression analysis of Li/Mg ratios and temperature ($r = -0.96$, $p(a) < 0.01$, $n = 218$) (1995 to 2013); e, reconstructed SSTs by each calibration. Error bars in a and b are 2σ external reproducibility errors for each elemental ratio, while in e the temperature errors are estimated from the 95% prediction intervals for each linear regression. The pink lines in c and d indicate the 95% prediction intervals. (For interpretation of the references to color in this figure legend, the reader is referred to the web version of this article.)

elements (e.g. Sr, Li, and B) and calcification rate, we suggest that this may be related to organic contamination effects. Therefore, this data was excluded from the temperature calibration.

To establish the Me/Ca-temperature relationship, the maximum Sr/Ca values were matched to the minimum temperature and the minimum Sr/Ca values were matched to the maximum temperature. Assuming linear growth between the summer maximums and winter minimums, the intervening SST can then be correlated with the interpolated Sr/Ca ratios. Using this approach, we performed linear regression between Sr/Ca and SST, yielding a regression equation of Sr/Ca (mmol/mol) = (−0.035 ± 0.002) × SST (°C) + (9.905 ± 0.024) ($r = -0.94$, $p(a) < 0.01$, n = 238; Fig. 2c) with the slope and intercept errors being estimated from the 95% prediction interval. The Sr/Ca-temperature sensitivity of ~0.035 mmol/mol/°C obtained is lower than that found in most tropical corals (average at ~0.047 mmol/mol/°C; D'Olivo et al., 2018), possibly reflecting reduced temperature sensitivity of coral Sr/Ca proxy in such a highly fluctuating and thermal intensive environment. Significant linear regressions were also found between Li/Mg ratios versus SST, producing the equation: Li/Mg (mmol/mol) = (−0.050 ± 0.001) × SST (°C) + (2.712 ± 0.026) ($r = -0.96$, $p(a) < 0.01$, n = 218; Fig. 2d). These equations were used to calculate Sr/Ca-SSTs and Li/Mg-SSTs, exhibiting parallel variations with the adjusted OISST (Fig. 2e), confirming the fidelity of both coral Sr/Ca and Li/Mg thermometers for this naturally extreme environment. The Li/Mg-SST calibration was further compared with the reported multispecies Li/Mg-temperature calibration (Fowell et al., 2016; Marchitto et al., 2018; Montagna et al., 2014), and found to broadly fit the exponential trend (Fig. S4), yielding a revised exponential regression: Li/Mg = 5.53exp(−0.051 × T) ($r = -0.98$, $p(a) < 0.01$, $n = 299$). The derived multispecies Li/Mg-SST, however, failed to capture the winter temperature (Fig. S4) and thus was not used in our study. The site-specific temperature calibrations were then used for annual SSTs reconstruction, with the average of paired Sr/Ca-SSTs and Li/Mg-SSTs used to represent annual SST variations (Fig. 3) which potentially reduces single-proxy uncertainties (D'Olivo et al., 2018).

4.2. Ocean warming in the nearshore Kimberley

Coral-derived annual SSTs showed a long-term trend (~0.009 ± 0.003 °C/yr) towards warmer temperatures over the period of 1919 to 2015 consistent with the satellite observation (~0.009 ± 0.001 °C/yr) (Fig. 3a), though the correlation between the coral reconstructed SST and ERSSTv4 (Huang et al., 2014) is generally weak ($r = +0.22$, $p(a) < 0.05$, $n = 97$) which is likely due to that the grid location of the satellite SST used here is ~60 km off the study site. When normalized to the period from 1971 to 2000, the annual temperature demonstrates positive anomalies in recent decades (1987 to 2015) with an average anomaly of ~0.45 °C (Fig. 3b). This long-term warming in the nearshore Kimberley region agrees with the other coral-based SST reconstructions in the Indian Ocean (Zinke et al., 2008,

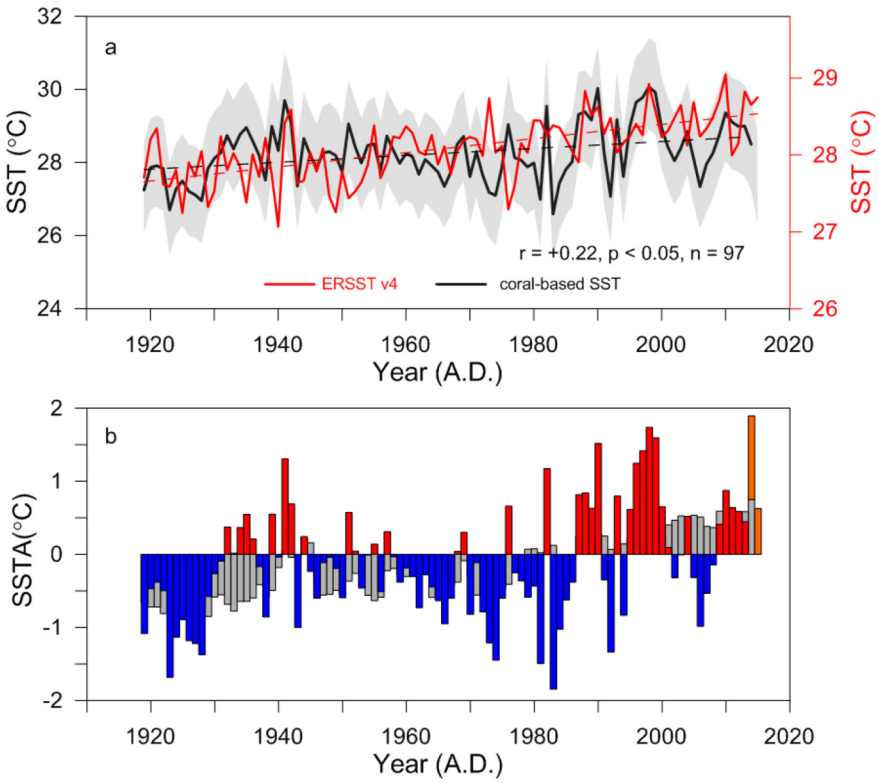

Fig. 3. Annual temperature records in the nearshore Kimberley: a, coral-based SST reconstruction and satellite SST for study area (16°S, 124°E) from extended reconstructed sea surface temperature: ERSST. v4, (Huang et al., 2014). The shaded areas indicate the temperature reconstruction errors that estimated from the prediction interval for Me/Ca-T calibration. Dashed lines indicate the long-term trend for each record (p(a) > 0.05). b, Reconstructed-SST anomalies (SSTA) (blue bars for negative anomalies and red for positive anomalies) against the average global SSTA (grey bars, data from ERSST. v4). Anomalies were calculated for the reference period of 1971 to 2000. The orange bars stand for the temperature anomaly calculated from Sr/Ca-SST excluding the aberrant Li/Mg values from 2014 to 2015. (For interpretation of the references to color in this figure legend, the reader is referred to the web version of this article.)

2014), and the overall increase in the SST of world's oceans (Huang et al., 2014) as a result of global warming. Compared with the general warming trend for global coral reefs (0.20 ± 0.11 °C/decade, 1985–2012, Heron et al., 2016), the trend in the King Sound falls within the upper part of the global range (0.28 ± 0.11 °C/decade, 1971–2014), and is distinctly higher than that reported for the global ocean waters (0.10–0.12 °C/decade, 1971–2010, Hartmann et al., 2013; Rhein et al., 2013). Further, the warming trend on seasonal timescales was also significant (p(a) < 0.05), with the SST warming of 0.05 ± 0.01 °C/yr in summers (2000–2015, Fig. 5a). Superimposed on this warming trend are significant inter-annual to decadal fluctuations which appear to have increased in amplitude after the 1970s (Fig. 3a). These findings suggest that under global climate change the naturally extreme Kimberley region has been undergoing both progressive long-term as well as pulsed warming events, which together are exacerbating the already extreme environmental conditions to which corals in the Kimberley region are being subjected to.

4.3. Seasonal variation in the CF carbonate chemistry

Monthly $\delta^{11}B$ and B/Ca time series (from 2008 to 2015) exhibited pronounced seasonal cycles in phase with Sr/Ca and Li/Mg ratios, and generally appeared to show an upward trend (Fig. S5). The $\delta^{11}B$ values varied from 23.15 to 25.64‰, with an average seasonal amplitude of typically > 1‰. When translated into pH_{cf} using Eq. (1), it shows that pH_{cf} in the calcifying fluid was elevated by ~0.4 pH Units compared to seawater pH (pH_{sw}; estimated from $pH_{sw} = -0.011T + 8.31$, details are given in electronic supplementary material), and varied seasonally from 8.34 to 8.60 in an opposing sense with temperature (Fig. 4) consistent with previous studies (D'Olivo and McCulloch, 2017; McCulloch et al., 2017). The seasonal variability of pH_{cf} is much larger than that expected from artificial experiments ($pH_{cf} = 0.32pH_{sw} + 5.95$, McCulloch et al., 2012a,b; Trotter et al., 2011) which show a much-subdued variation in pH_{cf} (Fig. 4c, dashed line). Skeletal B/Ca ratios also fluctuated seasonally, which converted to significant variations in DIC_{cf} from ~3592 to ~4679 μmol/kg. Compared with the measured seawater DIC (DIC_{sw}) (~1850 to ~1882 μmol/kg, Dandan et al., 2015), DIC_{cf} was elevated by ~2- to 2.6-fold (Fig. 4b), corroborating significant contribution from metabolic CO_2 to coral calcification (Erez, 1978; Furla et al., 2000). Enrichment in both DIC_{cf} and pH_{cf} leads to elevated aragonite saturation state in the calcifying site with Ω_{cf} varying seasonally from ~13 to ~16 and being ~ × 4 to × 5 higher than that of ambient seawater (Fig. 4d). Such features are similar to those found in corals growing in more typical tropical oceans (McCulloch et al., 2017), emphasizing the inherent commonality of the interactions between coral metabolism and internal carbonate chemistry. Importantly, this also suggests that such interactions between coral metabolism and calcifying fluid compositions as exhibited in Kimberley coral are maintained at 'normal levels' even under a highly fluctuating extreme temperature environment.

Although the up-regulated coral internal carbonate chemistry is not compromised by the extreme temperatures of the Kimberley region, we note that DIC_{cf} has decreased by ~10% from ~2008 to 2015 (Fig. 4b). The magnitude of the DIC_{cf} decrease (~500 μmol/kg) is significantly larger than changes in seawater DIC_{sw} (Dandan et al., 2015), and is indicative of a decline in the coral's ability to concentrate DIC in the calcifying fluid. Furthermore, DIC_{cf} reduction occurred in both warm and cooler seasons, accompanied by rapid summer warming and relatively stable winter temperatures (Fig. 5). The reverse trend in DIC_{cf} and temperature found for the summer data (Fig. 5) contrasts to the normal scenarios observed on seasonal timescales where higher temperature appear to promote greater production of metabolic CO_2, resulting in higher DIC_{cf} (Fig. 4). Therefore, the decline in DIC_{cf} is likely the result of reduced supply of metabolic CO_2 suggesting that recent warming has partially suppressed the metabolism of the coral or the zooxanthellae. This is consistent with the observations since 2002 of increased thermal stress, where the monthly summer water temperature in Cygnet Bay has frequently exceeded the maximum monthly mean (MMM, 31 °C, Schoepf et al., 2015) (Fig. 2), and unprecedented regional mass bleaching occurred in the nearshore Kimberley in 2016 (Le Nohaïc et al., 2017). Nevertheless, it seems that pH up-regulation is minimally, if at all, affected by the increased temperature, since pH_{cf}

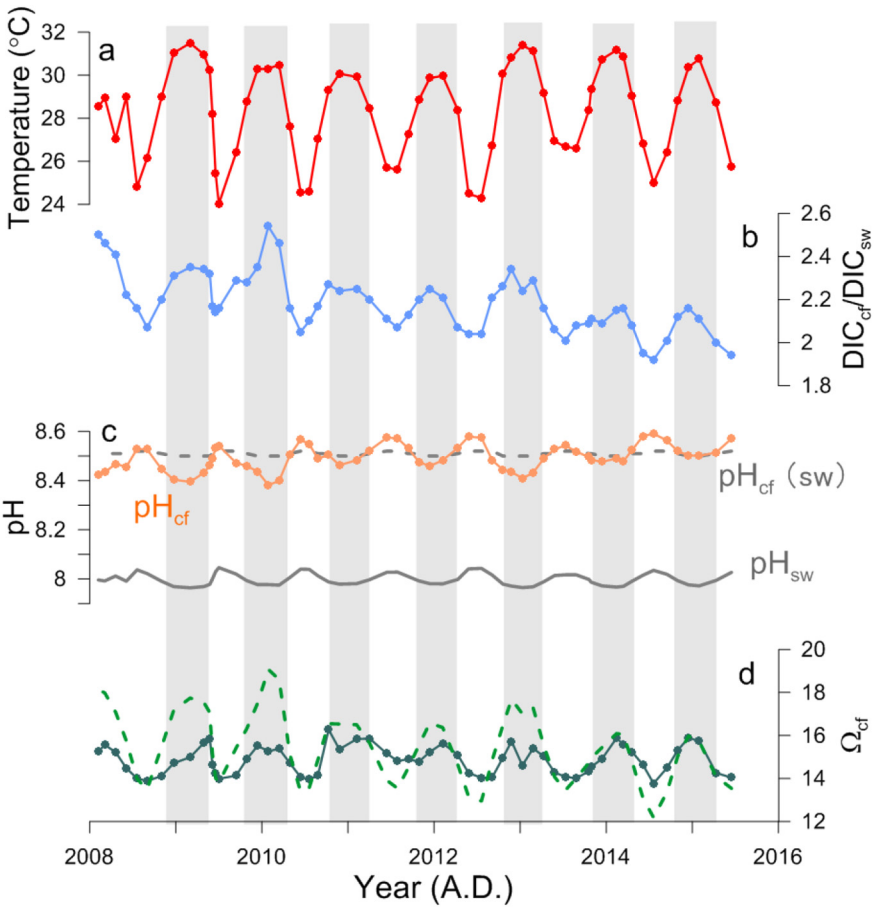

Fig. 4. Seasonal variations of temperature and coral CF carbonate chemistry: a, reconstructed-SSTs; b, DIC_{cf}/DIC_{sw}; c, pH_{cf} and pH_{sw}; d, aragonite saturation state (Ω_{cf}). Dashed lines indicate parameters calculated according to less variable pH_{cf}(sw) derived from the artificial experiments that pH_{cf} (sw) = $0.32pH_{sw}$ + 5.95 (McCulloch et al., 2012a,b; Trotter et al., 2011). Grey bars highlight the summer months.

still remains at an elevated level and shows an increasing trend in response to decreased metabolic DIC input (Fig. 5). Therefore, saturation state and calcification rate exhibit only relatively small disturbances from increasing temperature (Fig. 5). This is consistent with the previous observations in both field and culture experiments that corals possess the ability to regulate CF carbonate chemistry to maintain favorable calcification environment under extreme condition of temperature or seawater carbonate chemistry (Comeau et al., 2018; Ross et al., 2018).

4.4. Long-term variations in the CF carbonate chemistry

On the annual timescales, skeletal $\delta^{11}B$ and B/Ca time series were dominated by significant inter-annual and inter-decadal variations (Fig. S5). When calculated using Eqs. (1) and (2), the resultant DIC_{cf} and pH_{cf} exhibit antithetical variations like those observed on seasonal timescales (Fig. 6). The annual variability of DIC_{cf} is subdued compared to that on seasonal timescales, except a significant enhancement occurring around the 1990s (Fig. 6). Generally, the long-term trend of DIC_{cf} seems to follow the temperature, showing a marginal increase from the 1920s to the present, while in certain periods DIC_{cf} shows opposite variations with the temperature, especially during the recent decades. Therefore, the overall relationship between annual DIC_{cf} and temperature is weak, with a correlation coefficient of +0.31 (p(a) < 0.05; n = 96; Table S2), significantly lower than that on seasonal timescales (r = +0.60; p (a) < 0.05; n = 58; Table S2). In contrast to DIC_{cf}, pH_{cf} shows a long-term decreasing trend on the annual timescales, with a significant inverse relationship with DIC_{cf} (r = −0.87; p(a) < 0.05; n = 96) which is consistent with the strong seasonal inter-relationship between them. Therefore, the antithetical variations in DIC_{cf} and pH_{cf} are key to the maintenance of a relatively stable Ω_{cf} and hence calcification rate (Fig. 6).

4.5. Coral calcification under climate change

Although the SST in King Sound exhibited a clear warming trend, no significant trend (increase or decrease) was found for coral calcification rate (or annual linear extension rate) over the past century, with the values fluctuating within a normal range from ~1.2 to 1.6 g cm^{-2} yr^{-1} (Fig. 6). As discussed previously DIC_{cf}, however, was apparently affected by temperature increases (Figs. 4 & 6). In the long term, annual DIC_{cf} maybe expected to increase with the warming, assuming that temperature increases within the coral tolerance range would promote enhanced metabolic CO_2 production and thereby DIC_{cf}. However, once the temperature exceeds a critical threshold, coral metabolism and coral's ability to concentrate DIC_{cf} for calcification would be suppressed. For example, from 2008 to 2015, the repeated occurrence of abnormally warm summer temperature (above MMM) has apparently compromised the supply of metabolic CO_2 to coral calcifying fluid, causing a persistent decline in DIC_{cf}. This signifies that increasing water temperature in the nearshore Kimberley may have already reached a critical threshold such that enhanced summer warming is now adversely affecting coral symbiosis.

In contrast, annual pH_{cf} shows an overall decreasing trend while the DIC_{cf} and temperature increase. This long-term pH_{cf} reduction has also been observed for many corals in different reef environments (D'Olivo et al., 2015; Fowell et al., 2018; Goodkin et al., 2015; Kubota et al., 2017; Wei et al., 2009; Wu et al., 2018), with the amplitude comparable or often greater than the well-acknowledged centurial decrease in pH_{sw} (~0.1). For this reason, it has typically been assumed that coral internal pH_{cf} reduction is possibly a result of ocean acidification (D'Olivo et al., 2015; Fowell et al., 2018; Kubota et al., 2017; Wei et al., 2009; Wu

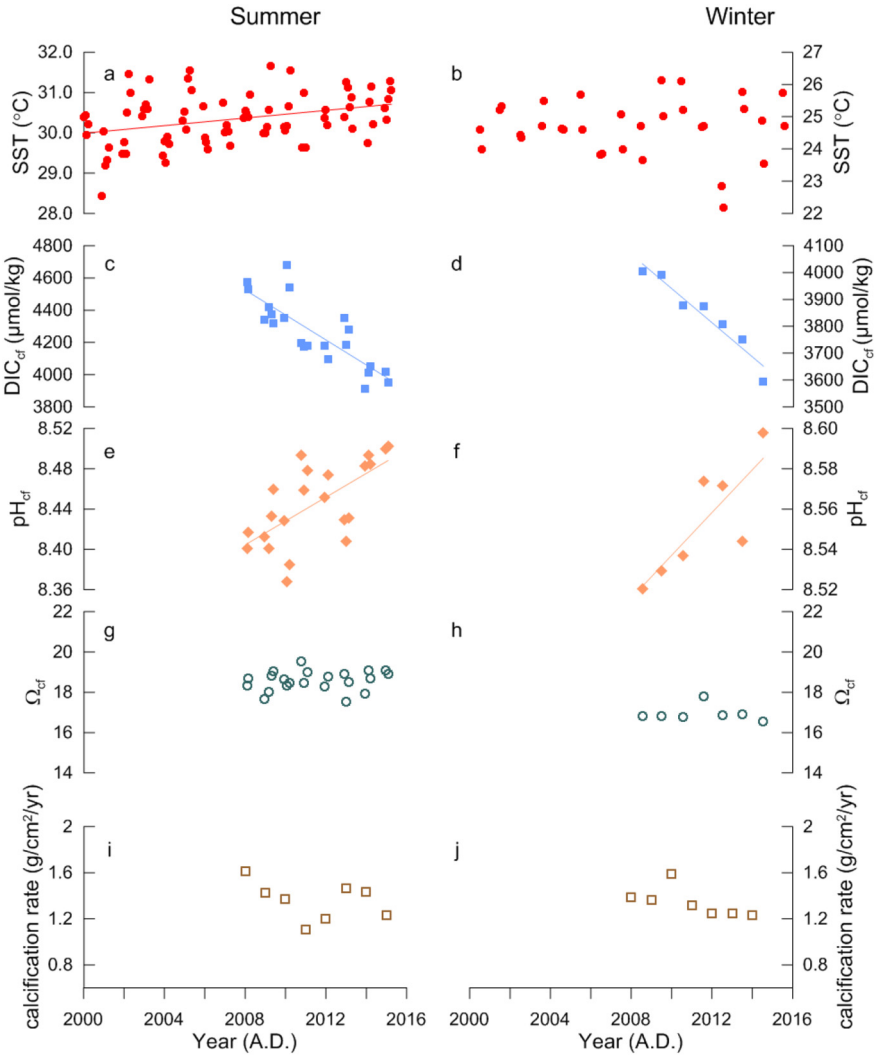

Fig. 5. Trends in summer (December to March) and winter (June to July) SST and coral CF carbonate chemistry: a–b, adjusted OISST; c–d, DIC_{cf}; e–f, pH_{cf}; g–h, Ω_{cf}; i–j: calcification rate. Linear regressions included when significant (p(a) > 0.05).

et al., 2018). To evaluate the long-term impact of pH_{sw} on coral pH_{cf} in the Kimberley coral, pH_{sw} variation was extracted from the annual pH_{cf} records (see details in electronic supplementary material) (Fig. 6c, grey line). The resultant pH_{sw} is characterized by inter-annual to decadal variations and exhibits a slight secular decreasing trend with the decline rate of ~0.007 ± 0.003 pH unit per decade, falling within the lower part of the modern observed ocean acidification rate range for the open ocean (varying from 0.013 ± 0.003 to 0.026 ± 0.006 pH unit per decade; Bates et al., 2014). In addition, pH_{cf} mimics the variation in pH_{sw}, implying that on the annual timescales pH_{sw} is the primary driver for pH_{cf}, possibly due to the relatively small temperature effect from global warming compared to seasonal timescales.

Although the coral is subject to both ocean warming and acidification, the observed long-term DIC_{cf} increase and pH_{cf} decrease seem to counteract the adverse impact of climate change on coral calcification. Therefore, the calcification rate calculated by the IpHRAC model exhibits relatively stable rates on the annual timescales, consistent with the measured rate of calcification (Fig. 6e). Despite that the measured and calculated rates exhibit sub-parallel variations, the calculated IpHRAC model rate is generally lower compared to that measured (Fig. 6e). This may be attributed to limitations in the accuracy of inorganic calcification rate parameters, but also indicates that calcification is not simply an inorganically controlled process but also subject to strong biological or physico-chemical controls. Recent studies have shown that although an optimum threshold of Ω_{cf} is required for coral calcification to occur, calcification rate is not directly determined by Ω_{cf} as expected from inorganic $CaCO_3$ precipitation (Comeau et al., 2018; D'Olivo and McCulloch, 2017; Ross et al., 2018; Schoepf et al., 2017). Additionally, skeletal organic matrix also play important roles in coral calcification, and calcification rates are strongly dependent on the coral architecture, in particular the effective surface area over which symbionts are distributed (Cuif et al., 1996; Teng et al., 1998; Von Euw et al., 2017). Therefore, it is not surprising that there can be large offsets between the calculated and the measured calcification rate.

Furthermore, measured versus IpHRAC calculated rates of calcification show divergent variations in certain periods, especially during short warming events. For instance, during the early 1990s coral calcification was suppressed despite the predicted calcification rate being increased. Similarly, during the recent warming (from 2005 onward), calcification rate decreased contrary to the predicted increase. These all indicate that the responses of coral calcification to environment changes are biologically limited instead of directly controlled by the thermodynamics of inorganic precipitation alone. This again corroborates that elevated 'threshold' levels of Ω_{cf} being an essential pre-requisite for calcification, is not necessarily rate limiting (D'Olivo and McCulloch, 2017; Ross et al., 2018). Clearly other physiologically dependent factors such as rates of production metabolites or DIC would be rate limiting especially under conditions of increased thermal stress.

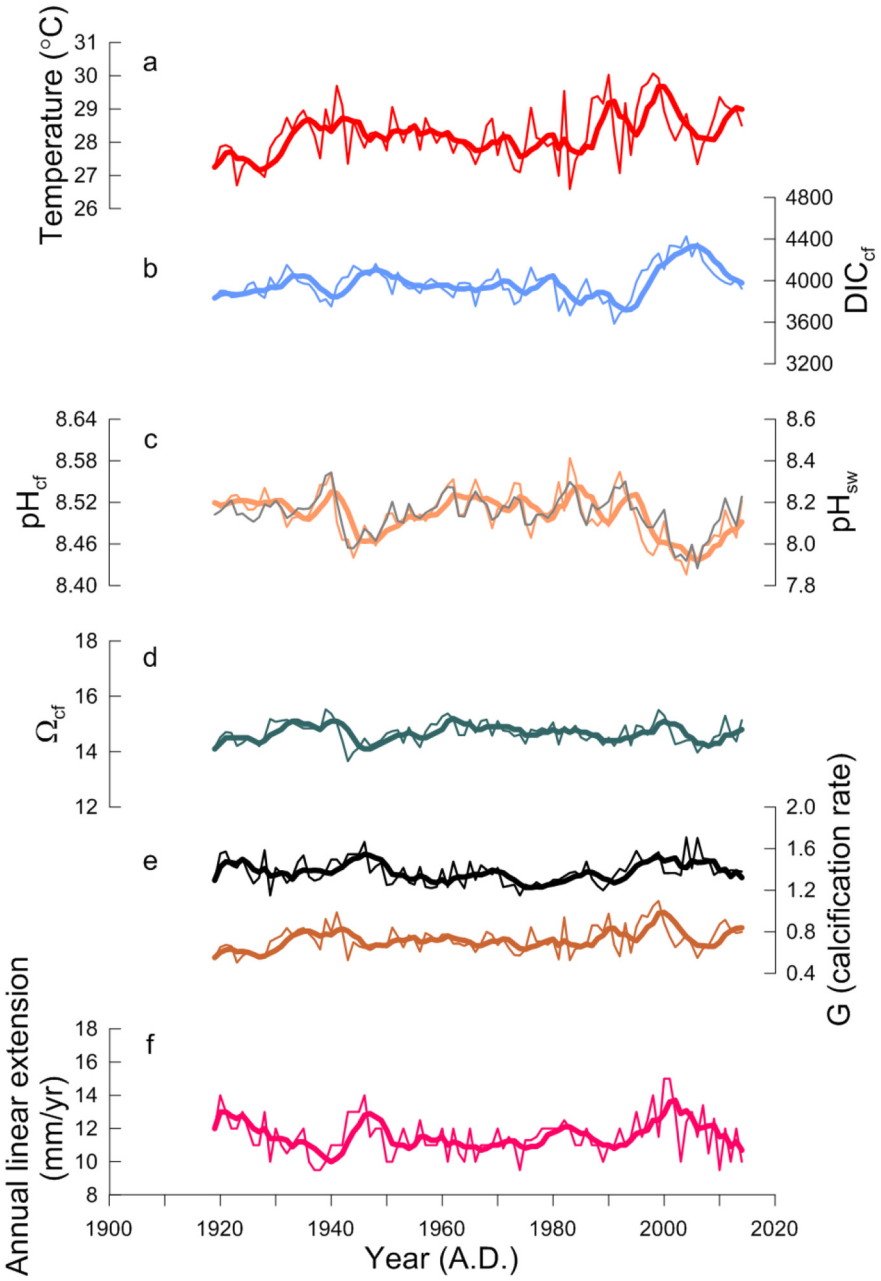

Fig. 6. Annual variations of coral CF carbonate chemistry and the estimated pH_{sw}: a, coral-based SST; b, DIC_{cf}; c, pH_{cf} (orange) and the reconstructed pH_{sw} (grey); d, Ω_{cf}; e, theoretical calcification rate (G, brown) and the measured calcification rate (black); f, annual linear extension rate. Bold lines represent 5-year running averages. (For interpretation of the references to color in this figure legend, the reader is referred to the web version of this article.)

5. Conclusions

Over the past century, the nearshore Kimberley has experienced a gradual increase as well as enhanced annual variation amplitude of temperature, with an accelerated warming trend evident in the recent decades possibly linked to elevated levels of thermal stress on corals. Despite higher levels of thermal stress, typical seasonal variations in CF carbonate chemistry, i.e. DIC_{cf}, pH_{cf}, Ω_{cf}, were observed, similar to that found in more typical tropical coral reef environment, confirming the inherent commonality in the interaction between coral metabolism and internal carbonate chemistry. However, during the most recent period (2008 to 2015) characterized by accelerated summer warming, we find coral DIC_{cf} has declined. This is a likely early indicator of enhanced thermal stress adversely impacting coral metabolism. However, coral pH_{cf} still remained at an elevated level even under the influence of ocean acidification helping to keep elevated and near constant levels of Ω_{cf}, highlighting the ability of coral to continue to manipulate the internal carbonate chemistry for calcification. As a result, coral calcification rate has remained relatively stable with no clear effects by climate change yet distinguishable.

Acknowledgements

The authors would like to thank Anne-Marin Nisumaa-Comeau and Dr. Kai Rankenburg for their assistance with the geochemical analysis. This research was supported by funding provided by an ARC Laureate Fellowship (LF120100049) awarded to Professor Malcolm McCulloch and the ARC Centre of Excellence for Coral Reef Studies (CE140100020) and financial support from the Western Australian Marine Science Institute (WAMSI). X.C. thanks the funding support

from the UCAS (UCAS Joint PhD Training Program) which supported her one-year academic visit at the UWA, and financial support from the National Key Research and Development Program of China (2016YFA0601204), and the National Natural Science Foundation of China (41803017, 41722301). This is contribution No. IS-2695 from GIG-CAS.

Data availability

Datasets for this article have been uploaded as the electronic supplementary files.

Appendix A. Supplementary data

Supplementary data to this article can be found online at https://doi.org/10.1016/j.palaeo.2019.04.033.

References

Bates, N.R., Astor, Y.M., Church, M.J., Currie, K., Dore, J.E., González-Dávila, M., Lorenzoni, L., Muller-Karger, F., Olafsson, J., Santana-Casiano, J.M., 2014. A time-series view of changing ocean chemistry due to ocean uptake of anthropogenic CO2 and ocean acidi cation. Oceanography 27 (1), 126–141. https://doi.org/10.5670/oceanog.2014.16.

Burton, E.A., Walter, L.M., 1987. Relative precipitation rates of aragonite and Mg calcite from seawater: temperature or carbonate ion control? Geology 15 (2), 111–114. https://doi.org/10.1130/0091-7613.

Cai, W., Borlace, S., Lengaigne, M., van Rensch, P., Collins, M., Vecchi, G., et al., 2014. Increasing frequency of extreme El Niño events due to greenhouse warming. Nat. Clim. Chang. 4, 111–116. https://doi.org/10.1038/nclimate2100.

Cantin, N.E., Cohen, A.L., Karnauskas, K.B., Tarrant, A.M., McCorkle, D.C., 2010. Ocean warming slows coral growth in the central Red Sea. Science 329 (5989), 322–325. https://doi.org/10.1126/science.1190182.

Clarke, H., D'Olivo, J.P., Falter, J., Zinke, J., Lowe, R., McCulloch, M., 2017. Differential response of corals to regional mass-warming events as evident from skeletal Sr/Ca and Mg/Ca ratios. Geochem. Geophys. Geosyst. 18, 1794–1809. https://doi.org/10.1002/2016GC006788.

Cohen, A.L., McConnaughey, T.A., 2003. Geochemical perspectives on coral mineralization. Rev. Mineral. Geochem. 54 (1), 151–187.

Comeau, S., Cornwall, C.E., DeCarlo, T.M., Krieger, E., McCulloch, M.T., 2018. Similar controls on calcification under ocean acidification across unrelated coral reef taxa. Glob. Chang. Biol. 24 (10), 4857–4868. https://doi.org/10.1111/gcb.14379.

Cooper, T.F., De'Ath, G., Fabricius, K.E., Lough, J.M., 2008. Declining coral calcification in massive Porites in two nearshore regions of the northern Great Barrier Reef. Glob. Chang. Biol. 14 (3), 529–538. https://doi.org/10.1111/j.1365-2486.2007.01520.x.

Cooper, T.F., O'Leary, R.A., Lough, J.M., 2012. Growth of Western Australian corals in the Anthropocene. Science 335 (6068), 593–596. https://doi.org/10.1126/science.1214570.

Cuif, J.-P., Dauphin, Y., Denis, A., Gautret, P., Marin, F., 1996. The organomineral structure of coral skeletons: a potential source of new criteria for Scleractinian taxonomy, Bulletin de l'Institut Océanographique. Monaco 14 (4), 359–367.

Cuny-Guirriec, K., Douville, E., Reynaud, S., Allemand, D., Bordier, L., Canesi, M., et al. (2019), Coral Li/Mg thermometry: caveats and constraints, Chemical Geology, accepted.

Dandan, S.S., Falter, J.L., Lowe, R.J., McCulloch, M.T., 2015. Resilience of coral calcification to extreme temperature variations in the Kimberley region, northwest Australia. Coral Reefs 34 (4), 1151–1163. https://doi.org/10.1007/s00338-015-1335-6.

De'ath, G., Lough, J.M., Fabricius, K.E., 2009. Declining coral calcification on the Great Barrier Reef. Science 323 (5910), 116–119.

DeCarlo, T.M., D'Olivo, J.P., Foster, T., Holcomb, M., Becker, T., McCulloch, M.T., 2017. Coral calcifying fluid aragonite saturation states derived from Raman spectroscopy. Biogeosciences 14, 5253–5269. https://doi.org/10.5194/bg-14-5253-2017.

Dickson, A.G., 1990a. Standard potential of the reaction: AgCl(s) + 12H2(g) = Ag (s) + HCl(aq), and and the standard acidity constant of the ion HSO4− in synthetic sea water from 273.15 to 318.15 K. J. Chem. Thermodyn. 22 (2), 113–127. https://doi.org/10.1016/0021-9614(90)90074-Z.

Dickson, A.G., 1990b. Thermodynamics of the dissociation of boric acid in synthetic seawater from 273.15 to 318.15 K. Deep Sea Research Part A. Oceanographic Research Papers 37 (5), 755–766. https://doi.org/10.1016/0198-0149(90)90004-F.

Dickson, A.G., Millero, F.J., 1987. A comparison of the equilibrium constants for the dissociation of carbonic acid in seawater media. Deep Sea Research Part A. Oceanographic Research Papers 34 (10), 1733–1743. https://doi.org/10.1016/0198-0149(87)90021-5.

D'Olivo, J.P., McCulloch, M.T., 2017. Response of coral calcification and calcifying fluid composition to thermally induced bleaching stress. Sci. Rep. 7 (1), 2207. https://doi.org/10.1038/s41598-017-02306-x.

D'Olivo, J.P., McCulloch, M.T., Judd, K., 2013. Long-term records of coral calcification across the central Great Barrier Reef: assessing the impacts of river runoff and climate change. Coral Reefs 32 (4), 999–1012. https://doi.org/10.1007/s00338-013-1071-8.

D'Olivo, J.P., McCulloch, M.T., Eggins, S.M., Trotter, J., 2015. Coral records of reef-water pH across the central Great Barrier Reef, Australia: assessing the influence of river runoff on inshore reefs. Biogeosciences 12 (4), 1223–1236. https://doi.org/10.5194/bg-12-1223-2015.

D'Olivo, J.P., Sinclair, D.J., Rankenburg, K., McCulloch, T.M., 2018. A universal multi-trace element calibration for reconstructing sea surface temperatures from long-lived Porites corals: removing 'vital effects'. Geochemica et Cosmochimica Acta 239, 109–135. https://doi.org/10.1016/j.gca.2018.07.035.

Duprey, N., Boucher, H., Jiménez, and Carlos. (2012), Digital correction of computered X-radiographs for coral densitometry, Jounral of Experimental Marine Biology and Ecology, 438(30), 94–92, doi: 10.1016/j.jembe.2012.09.007.

Erez, J., 1978. Vital effect on stable-isotope composition seen in foraminifera and coral skeletons. Nature 273 (5659), 199–202.

Foster, G.L., Ni, Y., Haley, B., Elliott, T., 2006. Accurate and precise isotopic measurement of sub-nanogram sized samples of foraminiferal hosted boron by total evaporation NTIMS. Chem. Geol. 230 (1–2), 161–174. https://doi.org/10.1016/j.chemgeo.2005.12.006.

Foster, G., von Strandmann, P.A.E.P., Rae, J., 2010. Boron and magnesium isotopic composition of seawater. Geochem. Geophys. Geosyst. 11 (8), Q08015. https://doi.org/10.1029/2010GC003201.

Fowell, S.E., Sandford, K., Stewart, J.A., Castillo, K.D., Ries, J.B., Foster, G.L., 2016. Intrareef variations in Li/Mg and Sr/Ca sea surface temperature proxies in the Caribbean reef-building coral Siderastrea siderea. Paleoceanography 31 (10), 1315–1329. https://doi.org/10.1002/2016PA002968.

Fowell, S.E., Foster, G.L., Ries, J.B., Castillo, K.D., de la Vega, E., Tyrrell, T., Donald, H.K., Chalk, T.B., 2018. Historical trends in pH and carbonate biogeochemistry on the Belize Mesoamerican Barrier Reef System. Geophycial Research Letters 45, 3228–3237. https://doi.org/10.1002/2017GL076496.

Furla, P., Galgani, I., Durand, I., Allemand, D., 2000. Sources and mechanisms of inorganic carbon transport for coral calcification and photosynthesis. J. Exp. Biol. 203 (22), 3445–3457.

Gagan, M., Ayliffe, L., Beck, J., Cole, J., Druffel, E., Dunbar, R., Schrag, D., 2000. New views of tropical paleoclimates from corals. Quat. Sci. Rev. 19 (1), 45–64.

Gagnon, A.C., Adkins, J.F., Erez, J., 2012. Seawater transport during coral biomineralization. Earth Planet. Sci. Lett. 329–330, 150–161. https://doi.org/10.1016/j.epsl.2012.03.005.

Gonfiantini, R., Tonarini, S., Gröning, M., Adorni-Braccesi, A., Al-Ammar, A.S., Astner, M., et al., 2003. Intercomparison of boron isotope and concentration measurements. Part II: evaluation of results. Geostand. Newslett. 27 (1), 41–57. https://doi.org/10.1111/j.1751-908X.2003.tb00711.x.

Goodkin, N.F., Wang, B.-S., You, C.-F., Hughen, K.A., Grumet-Prouty, N., Bates, N.R., Doney, S.C., 2015. Ocean circulation and biogeochemistry moderate interannual and decadal surface water pH changes in the Sargasso Sea. Geophys. Res. Lett. 42, 4931–4939. https://doi.org/10.1002/2015GL064431.

Hartmann, D.L., Klein Tank, A.M.G., Rusticucci, M., Alexander, L.V., Brönnimann, S., Charabi, Y.A.R., et al., 2013. Observations: atmosphere and surface. In: Stocker, T.F. (Ed.), Climate Change 2013: The Physical Science Basis: Working Group I Contribution to the Fifth Assessment Report of the Intergovernmental Panel on Climate Change. vol. 9781107057999. Cambridge University Press, pp. 159–254. https://doi.org/10.1017/CBO9781107415324.008.

Hathorne, E.C., Gagnon, A., Felis, T., Adkins, J., Asami, R., Boer, W., et al., 2013. Interlaboratory study for coral Sr/Ca and other element/Ca ratio measurements. Geochem. Geophys. Geosyst. 14 (9), 3730–3750. https://doi.org/10.1002/ggge.20230.

Heron, S.F., Maynard, J.A., van Hooidonk, R., Eakin, C.M., 2016. Warming trends and bleaching stress of the world's coral reefs 1985–2012. Sci. Rep. 6, 38402. https://doi.org/10.1038/srep38402.

Holcomb, M., DeCarlo, T. M., Schoepf, V., Dissard, D., Tanaka, K., and McCulloch, M. (2015), Cleaning and pre-treatment procedures for biogenic and synthetic calcium carbonate powders for determination of elemental and boron isotopic compositions, Chem. Geol., 398(0), 11–21, doi: https://doi.org/10.1016/j.chemgeo.2015.01.019.

Holcomb, M., DeCarlo, T.M., Gaetani, G.A., McCulloch, M., 2016. Factors affecting B/Ca ratios in synthetic aragonite. Chem. Geol. 437, 67–76. https://doi.org/10.1016/j.chemgeo.2016.05.007.

Huang, B., Banzon, V.F., Freeman, E., Lawrimore, J., Liu, W., Peterson, T.C., et al., 2014. Extended Reconstructed Sea Surface Temperature version 4 (ERSST.v4): part I. Upgrades and intercomparisons. J. Clim. 28, 911–930. https://doi.org/10.1175/JCLI-D-14-00006.1.

Hughes, T.P., Kerry, J.T., Álvarez-Noriega, M., Álvarez-Romero, J.G., Anderson, K.D., Baird, A.H., et al., 2017. Global warming and recurrent mass bleaching of corals. Nature 543 (7645), 373–377. https://doi.org/10.1038/nature21707.

Klochko, K., Kaufman, A.J., Yao, W., Byrne, R.H., Tossell, J.A., 2006. Experimental measurement of boron isotope fractionation in seawater. Earth Planet. Sci. Lett. 248 (1–2), 276–285. https://doi.org/10.1016/j.epsl.2006.05.034.

Kubota, K., Yokoyama, Y., Ishikawa, T., Suzuki, A., Ishii, M., 2017. Rapid decline in pH of coral calcification fluid due to incorporation of anthropogenic CO2. Sci Rep-Uk 7 (1), 7694. https://doi.org/10.1038/s41598-017-07680-0.

Lazareth, C.E., Soares-Pereira, C., Douville, E., Brahmi, C., Dissard, D., Le Cornec, F., et al., 2016. Intra-skeletal calcite in a live-collected Porites sp.: impact on environmental proxies and potential formation process. Geochim. Cosmochim. Acta 176, 279–294. https://doi.org/10.1016/j.gca.2015.12.020.

Le Nohaïc, M., Ross, C.L., Cornwall, C.E., Comeau, S., Lowe, R., McCulloch, M.T., Schoepf, V., 2017. Marine heatwave causes unprecedented regional mass bleaching of thermally resistant corals in northwestern Australia. Sci. Rep. 7, 14999. https://doi.org/10.1038/s41598-017-14794-y.

Lough, J.M., Barnes, D.J., 1992. Comparisons of skeletal density variations in Porites from

the central Great Barrier Reef. J. Exp. Mar. Biol. Ecol. 155 (1), 1–25. https://doi.org/10.1016/0022-0981(92)90024-5.
Lough, J.M., Barnes, D.J., 1997. Several centuries of variation in skeletal extension, density and calcification in massive Porites colonies from the Great Barrier Reef: a proxy for seawater temperature and a background of variability against which to identify unnatural change. J. Exp. Mar. Biol. Ecol. 211 (1), 29–67. https://doi.org/10.1016/S0022-0981(96)02710-4.
Marchitto, T.M., Bryan, S.P., Doss, W., McCulloch, M.T., Montagna, P., 2018. A simple biomineralization model to explain Li, Mg, and Sr incorporation into aragonitic foraminifera and corals. Earth Planet. Sci. Lett. 481, 20–29. https://doi.org/10.1016/j.epsl.2017.10.022.
McCulloch, M.T., Tudhope, A.W., Esat, T.M., Mortimer, G.E., Chappell, J., Pillans, B., Chivas, A.R., Omura, A., 1999. Coral record of equatorial sea-surface temperatures during the penultimate deglaciation at Huon Peninsula. Science 283, 202–204. https://doi.org/10.1126/science.283.5399.202.
McCulloch, M., Trotter, J., Montagna, P., Falter, J., Dunbar, R., Freiwald, A., et al., 2012a. Resilience of cold-water scleractinian corals to ocean acidification: boron isotopic systematics of pH and saturation state up-regulation. Geochim. Cosmochim. Acta 87, 21–34. https://doi.org/10.1016/j.gca.2012.03.027.
McCulloch, M.T., Falter, J.L., Trotter, J., Montagna, P., 2012b. Coral resilience to ocean acidification and global warming through pH up-regulation. Nat. Clim. Chang. 2, 1–5. https://doi.org/10.1038/nclimate1473.
McCulloch, M.T., Holcomb, M., Rankenburg, K., Trotter, J.A., 2014. Rapid, high-precision measurements of boron isotopic compositions in marine carbonates. Rapid Commun. Mass Spectrom. 28 (24), 2704–2712. https://doi.org/10.1002/rcm.7065.
McCulloch, M.T., D'Olivo, J.P., Falter, J., Holcomb, M., Trotter, J.A., 2017. Coral calcification in a changing world and the interactive dynamics of pH and DIC upregulation. Nat. Commun. 8, 15686. https://doi.org/10.1038/ncomms15686.
Mehrbach, C., Culberson, C.H., Hawley, J.E., Pytkowicx, R.M., 1973. Measurement of the apparent dissociation constants of carbonic acid in seawater at atmospheric pressure 1. Limnol. Oceanogr. 18 (6), 897–907. https://doi.org/10.4319/lo.1973.18.6.0897.
Meibom, A., Cuif, J.-P., Houlbreque, F., Mostefaoui, S., Dauphin, Y., Meibom, K.L., Dunbar, R., 2008. Compositional variations at ultra-structure length scales in coral skeleton. Geochim. Cosmochim. Acta 72, 1555–1569. https://doi.org/10.1016/j.gca.2008.01.009.
Montagna, P., McCulloch, M., Douville, E., López Correa, M., Trotter, J., Rodolfo-Metalpa, R., et al., 2014. Li/Mg systematics in scleractinian corals: calibration of the thermometer. Geochim. Cosmochim. Acta 132, 288–310. https://doi.org/10.1016/j.gca.2014.02.005.
Mucci, A., Morse, J.W., 1983. The incorporation of Mg2+ and Sr2+ into calcite overgrowths: influences of growth rate and solution composition. Geochim. Cosmochim. Acta 47 (2), 217–233. https://doi.org/10.1016/0016-7037(83)90135-7.
Purcell, S., 2002. Intertidal reefs under extreme tidal flux in Buccaneer Archipelago. Western Australia, Coral Reefs 21 (2), 191–192. https://doi.org/10.1007/s00338-002-0223-z.
Reynolds, R.W., Smith, T.M., Liu, C., Chelton, D.B., Casey, K.S., Schlax, M.G., 2007. Daily high-resolution-blended analyses for sea surface temperature. J. Clim. 20 (22), 5473–5496. https://doi.org/10.1175/2007jcli1824.1.
Rhein, M., Rintoul, S.R., Aoki, S., Campos, E., Chambers, D., Feely, R., et al., 2013. Observations: ocean. In: Stocker, T.F. (Ed.), Climate Change 2013: The Physical Science Basis. Working Group I Contribution to the Fifth Assessment Report of the Intergovernmental Panel on Climate Change. vol. 9781107057999. Cambridge University Press, pp. 255–316.
Richards, Z.T., Garcia, R.A., Wallace, C.C., Rosser, N.L., Muir, P.R., 2015. A diverse assemblage of reef corals thriving in a dynamic intertidal reef setting (Bonaparte Archipelago, Kimberley, Australia). PLoS One 10, e0117791. https://doi.org/10.1371/journal.pone.0117791.
Ross, C.L., Schoepf, V., DeCarlo, T.M., McCulloch, M.T., 2018. Mechanisms and seasonal drivers of calcification in the temperate coral *Turbinaria reniformis* at its latitudinal limits. Proc. R. Soc. B Biol. Sci. 285, 20180215. https://doi.org/10.1098/rspb.2018.0215.
Rosser, N.L., Veron, J.E.N., 2011. Australian corals thriving out of water in an extreme environment. Coral Reefs 30 (1), 21. https://doi.org/10.1007/s00338-010-0689-z.
Schoepf, V., Stat, M., Falter, J.L., McCulloch, M.T., 2015. Limits to the thermal tolerance of corals adapted to a highly fluctuating, naturally extreme temperature environment. Sci. Rep. 5, 17639. https://doi.org/10.1038/srep17639.
Schoepf, V., Jury, C.P., Toonen, R.J., McCulloch, M.T., 2017. Coral calcification mechanisms facilitate adaptive responses to ocean acidification. Proc. R. Soc. B Biol. Sci. 284, 20172117. https://doi.org/10.1098/rspb.2017.2117.
Smith, S.V., Buddemeier, R.W., Redalje, R.C., Houck, J.E., 1979. Strontium-calcium thermometry in coral skeletons. Science 204 (4391), 404–407. https://doi.org/10.1126/science.204.4391.404.
Spalding, M.D., Brown, B.E., 2015. Warm-water coral reefs and climate change. Science 350 (6262), 769–771. https://doi.org/10.1126/science.aad0349.
Tanzil, J.T.I., Brown, B.E., Dunne, R.P., Lee, J.N., Kaandorp, J.A., Todd, P.A., 2013. Regional decline in growth rates of massive Porites corals in Southeast Asia. Glob. Chang. Biol. 19 (10), 3011–3023. https://doi.org/10.1111/gcb.12279.
Teng, H.H., Dove, P.M., Orme, C.A., De Yoreo, J.J., 1998. Thermodynamics of calcite growth: baseline for understanding biomineral formation. Science 282 (5389), 724–727. https://doi.org/10.1126/science.282.5389.724.
Trotter, J., Montagna, P., McCulloch, M., Silenzi, S., Reynaud, S., Mortimer, G., et al., 2011. Quantifying the pH 'vital effect' in the temperate zooxanthellate coral Cladocora caespitosa: validation of the boron seawater pH proxy. Earth Planet. Sci. Lett. 303 (3–4), 163–173. https://doi.org/10.1016/j.epsl.2011.01.030.
Von Euw, S., Zhang, Q., Manichev, V., Murali, N., Gross, J., Feldman, L.C., et al., 2017. Biological control of aragonite formation in stony corals. Science 356 (6341), 933–938. https://doi.org/10.1126/science.aam6371.
Wang, B.-S., You, C.-F., Huang, K.-F., Wu, S.-F., Aggarwal, S.K., Chung, C.-H., Lin, P.-Y., 2010. Direct separation of boron from Na- and Ca-rich matrices by sublimation for stable isotope measurement by MC-ICP-MS. Talanta 82 (4), 1378–1384. https://doi.org/10.1016/j.talanta.2010.07.010.
Wei, G., McCulloch, M.T., Mortimer, G., Deng, W., Xie, L., 2009. Evidence for ocean acidification in the Great Barrier Reef of Australia. Geochim. Cosmochim. Acta 73 (8), 2332–2346.
Wu, H.C., Dissard, D., Douville, E., Blamart, D., Bordier, L., Tribollet, A., et al., 2018. Surface ocean pH variations since 1689 CE and recent ocean acification in the tropical South Pacific. Nat. Commun. 9, 2543. https://doi.org/10.1038/s41467-018-04922-1.
Zeebe, R.E., Wolf-Gladrow, D.A., 2001. CO2 in Seawater: Equilibrium, Kinetics, Isotopes. Elsevier Science Limited.
Zinke, J., Pfeiffer, M., Timm, O., Dullo, W.C., Kroon, D., Thomassin, B.A., 2008. Mayotte coral reveals hydrological changes in the western Indian Ocean between 1881 and 1994. Geophys. Res. Lett. 35 (23), L23707. https://doi.org/10.1029/2008GL035634.
Zinke, J., Rountrey, A., Feng, M., Xie, S.P., Dissard, D., Rankenburg, K., et al., 2014. Corals record long-term Leeuwin current variability including Ningaloo Niño/Niña since 1795. Nat. Commun. 5. https://doi.org/10.1038/ncomms4607.